JACS
JOURNAL OF THE AMERICAN CHEMICAL SOCIETY
Communication
pubs.acs.org/JACS

Solid-State NMR Crystallography through Paramagnetic Restraints

Claudio Luchinat,*[,†,‡] Giacomo Parigi,[†,‡] Enrico Ravera,[†,‡] and Mauro Rinaldelli[†]

[†]Magnetic Resonance Center (CERM), University of Florence, via Sacconi 6, Sesto Fiorentino, Italy
[‡]Department of Chemistry, University of Florence, via della Lastruccia 3, Sesto Fiorentino, Italy

Supporting Information

ABSTRACT: Pseudocontact shifts (PCSs) measured by solid-state NMR spectroscopy (SS-NMR) on microcrystalline powders of a paramagnetic metalloprotein permit NMR crystallography. Along with other restraints for SS-NMR experiments, the protein molecular structure as well as the correct crystal packing are obtained.

NMR crystallography is rapidly gaining interest. For micro- and nanocrystalline powders of small molecules, it permits access to both the atomic details of the molecular structure and the crystal packing.[1−6] A small protein (GB1, 6 kDa) has also been recently tackled.[7,8] It is shown here that pseudocontact shifts (PCSs) are very suitable restraints for protein NMR crystallography.

PCSs are long-range structural restraints[9−13] that become available in the presence of a paramagnetic ion coordinated to the investigated molecule or attached to it with a paramagnetic tag.[14−18] In crystals, the presence of paramagnetic ions in neighboring molecules determines PCS values that are affected by both intramolecular and intermolecular contributions.[12,19,20] As a result, while intramolecular PCSs are valuable restraints for obtaining the molecular structure, intermolecular PCSs can provide information on the relative arrangement of the molecules within the crystal.[20] Indeed, PCSs have been recently used to perform NMR crystallography of small lanthanide chelates.[20]

For paramagnetic proteins, the two contributions to the total PCS can be separated using dilution of the paramagnetic molecules in combination with different labeling strategies.[21−25] Intramolecular PCSs were measured with this approach for the high-spin Co(II)-substituted protein matrix metalloproteinase 12 (CoMMP-12), a 17 kDa protein, for nuclei up to ∼20 Å from the metal ion.[19,22,26] The use of intramolecular PCSs coupled to distance restraints measured for the native Zn(II)-containing protein provided a protein structural family with reasonably high resolution.[26] The strength of using PCSs to help structure determination by solid-state NMR spectroscopy (SS-NMR) resides in the fact that PCSs are immediately available, while many distance restraints are initially ambiguous and can be introduced only after the first emerging structural family can be used to resolve ambiguities. A drawback is represented by the need to dilute the paramagnetic protein into a larger amount of the diamagnetic protein to ensure that the measured PCSs are all intramolecular. Thus, the concentration of the labeled species is low, resulting in a low signal-to-noise ratio. Furthermore, all of the information on the crystal lattice is lost. We show here, on the same metalloprotein system CoMMP-12, that total PCSs can be used as such on nondiluted systems and that a refinement scheme based on such PCS data and other intramolecular restraints is feasible for obtaining (1) the structure of the protein and (2) the crystal packing, once the cell parameters are available from powder X-ray diffraction (PXRD). Because of the higher signal-to-noise ratio, the number of measurable total PCSs (476)[27] is considerably larger than the number of intramolecular PCSs (319).[26] Solving protein structures through SS-NMR can be advantageous for those systems that cannot be solved through solution NMR, such as large proteins, membrane proteins, and fibrils. The present approach yields both the structure and the crystal packing in the case of microcrystalline proteins, even if the quality of the crystals may not be good enough to provide accurate X-ray structures; it can still yield structural information on systems with only short-range order, such as amyloid fibrils and other large biomolecular assemblies.

The rationale for this strategy to work is the fact that most PCSs are likely to be dominated by intramolecular rather than intermolecular contributions, allowing the latter to be considered a perturbation of the former. Accordingly, a two-step procedure has been designed: (1) From the very beginning of the structure calculations, an adjustable number of external metal ions are introduced together with the intramolecular metal ion. In this way, the relatively minor contribution of intermolecular PCSs is empirically taken into accounted, and the intramolecular contribution becomes accurate enough to permit the structure calculation. Each metal ion is described not only by its position but also by the orientation of the magnetic susceptibility tensor with axial and rhombic anisotropies ($\Delta\chi_{ax}$ and $\Delta\chi_{rh}$, respectively).[28] (2) In the case that PXRD data can provide accurate cell parameters, once the structure is obtained, the external metal ions introduced empirically can be substituted by the full crystal lattice of metalloprotein molecules, and the molecular structure is refined together with the crystal structure.

The following steps were thus implemented [details of the single steps are reported in the Supporting Information (SI)]:

(1) *Calculation of the molecular structure using total PCSs.*
- The total PCSs, together with dihedral angle restraints and the unambiguous distance restraints found initially, are used to perform ab initio structure calculations for the determination of the protein fold, including from the very beginning n + 1 independently positioned paramagnetic metal

Received: October 26, 2011
Published: March 6, 2012

dx.doi.org/10.1021/ja210079n | J. Am. Chem. Soc. 2012, 134, 5006−5009

ions (one intra- and n intermolecular). The number n can be empirically found as the minimum number of metal ions needed for the best reproduction of the experimental data [i.e., for which there is no significant further decrease in the target function (TF)].

- The obtained structural fold is used to iteratively resolve ambiguities in the NMR spectra and to determine additional distance restraints, similar to what has been shown to work in the case of purely intramolecular PCSs.[26]
- The values of the anisotropy parameters $\Delta\chi_{ax}$ and $\Delta\chi_{rh}$, which are initially set to literature values typical of the paramagnetic metal ion,[29] are refined by performing a grid search. The anisotropy parameters are thus fixed to the values providing the minimum value of the TF.

In the case of CoMMP-12, the total PCSs, the dihedral angle restraints, and the 240 unambiguous distance restraints found initially, used as upper distance limits (UPLs) between protein nuclei, provided a protein structure with the lowest TF when four paramagnetic metal ions were included (i.e., for n = 3) (Figure S1 in the SI; Table 1, entry 1). As expected, the obtained structural family permitted the determination of additional distance restraints (see the SI). The anisotropy parameters were then fixed to the refined values, which were $(9 \pm 1) \times 10^{-32}$ and $(-3.0 \pm 0.3) \times 10^{-32}$ m^3 for $\Delta\chi_{ax}$ and $\Delta\chi_{rh}$, respectively. By doing so, we could obtain a structure of approximately the same quality as the one previously obtained with intramolecular PCSs only: the 20 structures with the lowest TFs have a backbone (BB) root-mean-square deviation (RMSD) of 0.9 Å with respect to the mean, and the RMSD with respect to the X-ray structure is 1.4 Å (Table 1, entry 2; Figure 1).

Table 1. Structural Parameters for the MMP-12 Structures Calculated Using SS-NMR

			RMSD (Å)		
entry	model	TF (Å^2)	BB to mean	BB mean to X-ray[a]	secondary structure mean to X-ray[a]
1	240 UPLs + 476 PCSs, four independent metal ions[b]	2.97–7.09	4.3	4.5	2.2
2	727 UPLs + 476 PCSs, four independent metal ions	0.70–0.86	0.9	1.4	1.0
3	crystal ($P2_12_12$)	0.86–1.22	0.9	1.2	0.9
4	crystal ($P2_12_12_1$)	1.97–2.72	0.9	1.6	0.9
5	paramagnetically diluted protein[c]	2.66–4.22	1.0	1.3	0.9

[a]Structure 1RMZ. [b]Calculated with a different weight for PCSs and with the literature tensor. [c]Structure 2KRJ calculated by Bertini et al.[26] using only intramolecular PCSs and larger weights.

(2) *Calculation of the crystal structure using total PCSs.*

At this stage, the global information on the positions of all crystal mates should be added.

- For this final step, a crystallographic space group must be imposed. In X-ray crystallography, such information is usually extracted during the structural refinement,[30] and in the present case, we relied on the existing unit cell parameters from the single-crystal X-ray structure.[31] Obviously, a crystal structure is not available if one resorts to NMR crystallography, where microcrystalline powders are employed. However, a PXRD pattern is in principle enough to obtain the dimensions and shape of the unit cell.[32] Microcrystalline powders are frequently obtained in failed attempts to grow the desired crystals.[33] The unit cell dimensions extracted from PXRD patterns can be very accurate,[34] with a precision even higher than that usually achieved from single-crystal XRD.[33]
- Once the cell parameters have been determined, the correct symmetry must be identified. Structure calculations including all of the paramagnetic metal ions in the crystal must be then performed for each of the possible space groups.
- The implementation of the symmetry-generated PCSs is not straightforward and requires a substantial modification of the PARAMAGNETIC CYANA program.[35,36] A pseudoresidue is introduced to position freely the crystallographic origin and reference frame. The positions of the metal ions of neighboring molecules and the orientations of the corresponding magnetic susceptibility anisotropy tensors with respect to this crystallographic frame are obtained according to the symmetry rules. In turn, the position of the crystallographic frame is determined during the minimization by introducing into the TF the intermolecular contributions to the PCSs due to all the neighboring molecules in the crystal. It should

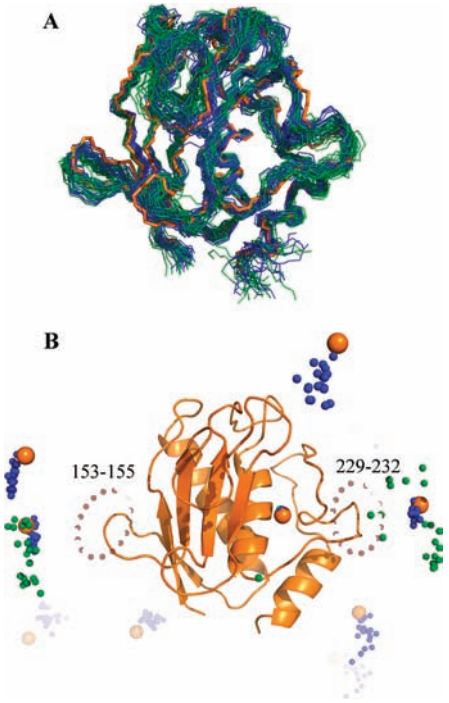

Figure 1. Family of MMP-12 structures calculated using four independently positioned metal ions (green) and metal ions positioned according to the imposed crystallographic symmetry (blue) superimposed on the X-ray structure (orange). (B) The positions of the metal ions in the three cases are shown, and the residue numbers of the residues closest to the external metal ions are indicated.

dx.doi.org/10.1021/ja210079n | J. Am. Chem. Soc. 2012, 134, 5006–5009

be noted that the introduction of the pseudoresidue mimicking the crystallographic frame reduces the number of degrees of freedom with respect to those present in step 1, in which there are $n > 1$ independently positioned paramagnetic metal ions. As for the main CYANA program, dynamics in torsion angle space requires the analytical definition of the first derivative of the intermolecular contributions to the PCSs with respect to the dihedral angles. The mathematical details are described in the SI, and the corresponding routines are available at http://www.cerm.unifi.it/softwares/cryana.

In the case of CoMMP-12, the good quality of the NMR spectra and the absence of signal doubling ensured a lack of crystal heterogeneity. The unit cell parameters are a = 69.194 Å, b = 62.564 Å, c = 37.262 Å, and $\alpha = \beta = \gamma = 90°$, indicating an orthorhombic symmetry.[31] Nine different orthorhombic symmetries are possible, differing by the number of molecules per unit cell (see the SI). The Matthews coefficient[37,38] indicated that it would be reasonable to expect four molecules per unit cell. Therefore, only the $P222$, $P222_1$, $P2_12_12$, and $P2_12_12_1$ space groups were allowed.

The first two symmetries ($P222$ and $P222_1$) did not provide any acceptable solutions because all of the calculated structures with low TFs showed severe compenetration among symmetry-related molecules (Figure S2). In the case of the $P2_12_12_1$ symmetry, non-compenetrating structures were calculated, but their TFs were >2 times larger than in the $P2_12_12$ case (entry 4 vs 3, respectively, in Table 1). Therefore, the experimental data strongly point to the $P2_12_12$ symmetry. The BB RMSD with respect to the mean was 0.9 Å, and the RMSD to the X-ray structure was 1.2 Å (Table 1, entry 3). These values are the same or slightly better than those previously obtained from intramolecular PCSs (Table 1, entry 5).[26] Therefore, total PCSs are at least as good as intramolecular PCS for structural purposes.[39] The agreement of the calculated PCS values for the nuclei of the different residues with the experimental data is shown in Figure S5.

Figure 2 shows the superposition of the lowest-TF structure with the X-ray structure, together with all surrounding symmetry-related molecules. The agreement is very good, showing that PCSs were indeed able to reconstruct the crystal with good accuracy once the cell parameters were available. This indicates that the intermolecular contributions to the PCSs are indeed able to locate the crystallographic origin and reference frame correctly. This achievement is quite striking, considering that no information on van der Waals attractive or repulsive potentials was included in the calculations. Finally, it is noteworthy that the structural family calculated with the crystallographic restraints showed a further non-negligible improvement with respect to the family calculated using independently positioned metal ions, as the BB RMSD with respect to the X-ray structure decreased from 1.4 to 1.2 Å (entries 2 and 3, respectively, in Table 1).

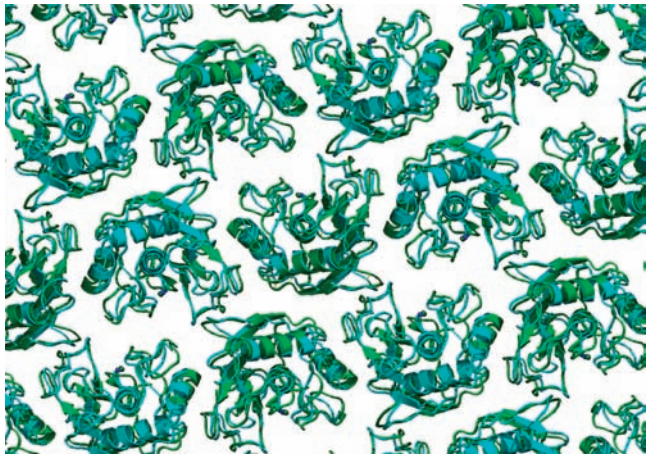

Figure 2. Superposition of the lowest-TF SS-NMR structure (cyan) with the X-ray structure (green) together with the crystal mates.

In conclusion, the protein structure and the crystal structure of the Co(II)-substituted MMP-12 could be calculated in two steps using total PCSs measured for the protein in the solid state, which are composed of intramolecular and intermolecular contributions, together with other distance restraints and dihedral angle restraints. A protein structure of good accuracy is obtained using the PCSs measured without any paramagnetic dilution and in the absence of PXRD data. If the cell parameters are known, the structure of the crystal can also be determined through the effect of the metal ions of neighboring molecules on the PCSs, and the molecular structure can be simultaneously refined.

■ ASSOCIATED CONTENT

Supporting Information

Experimental PCSs, procedure used in the calculations, inclusion of the intermolecular contributions to the PCSs from crystal-symmetry molecules in PARAMAGNETIC CYANA, and supporting figures. This material is available free of charge via the Internet at http://pubs.acs.org.

■ AUTHOR INFORMATION

Corresponding Author

luchinat@cerm.unifi.it

Notes

The authors declare no competing financial interest.

■ ACKNOWLEDGMENTS

Ivano Bertini and Stefano Mangani are acknowledged for several discussions. Anusarka Bhaumik (Rutgers University), Vito Calderone (CERM) and Moreno Lelli (Université de Lyon) are acknowledged for early discussions; Mauro Cremonini (Agilent Technologies, Italy), Gabriele Cavallaro and Antonio Rosato (CERM) are acknowledged for fruitful discussion about PARAMAGNETIC CYANA. This work has been supported by Ente Cassa di Risparmio, MIUR-FIRB contracts RBLA032ZM7, RBRN07BMCT, and by European Commission, contracts East-NMR n. 228461, WeNMR n. 261572, and Bio-NMR n. 261863.

■ REFERENCES

(1) Elena, B.; Emsley, L. *J. Am. Chem. Soc.* **2005**, *127*, 9140.
(2) Elena, B.; Pintacuda, G.; Mifsud, N.; Emsley, L. *J. Am. Chem. Soc.* **2006**, *128*, 9555.
(3) Webber, A. L.; Emsley, L.; Claramunt, R. M.; Brown, S. P. *J. Phys. Chem. A* **2010**, *114*, 10435.
(4) Bradley, J. P.; Velaga, S. P.; Antzutkin, O. N.; Brown, S. P. *Cryst. Growth Des.* **2011**, *11*, 3463.
(5) Dumez, J. N.; Emsley, L. *Phys. Chem. Chem. Phys.* **2011**, *13*, 7363.
(6) Geppi, M.; Mollica, G.; Borsacchi, S.; Veracini, C. A. *Appl. Spectrosc. Rev.* **2008**, *43*, 202.

(7) Nieuwkoop, A. J.; Rienstra, C. M. *J. Am. Chem. Soc.* **2010**, *132*, 7570.
(8) Bayro, M. J.; Debelouchina, G. T.; Eddy, M. T.; Birkett, N. R.; MacPhee, C. E.; Rosay, M. M.; Maas, W.; Dobson, C. M.; Griffin, R. G. *J. Am. Chem. Soc.* **2011**, *133*, 13967.
(9) Bertini, I.; Kursula, P.; Luchinat, C.; Parigi, G.; Vahokoski, J.; Willmans, M.; Yuan, J. *J. Am. Chem. Soc.* **2009**, *131*, 5134.
(10) Bertini, I.; Luchinat, C.; Parigi, G.; Pierattelli, R. *Dalton Trans.* **2008**, 3782.
(11) Pintacuda, G.; John, M.; Su, X. C.; Otting, G. *Acc. Chem. Res.* **2007**, *40*, 206.
(12) Bertini, I.; Luchinat, C.; Parigi, G. *Coord. Chem. Rev.* **2011**, *255*, 649.
(13) Schmitz, C.; Stanton-Cook, M. J.; Su, X. C.; Otting, G.; Huber, T. *J. Biomol. NMR* **2008**, *41*, 179.
(14) Su, X. C.; Man, B.; Beeren, S.; Liang, H.; Simonsen, S.; Schmitz, C.; Huber, T.; Messerle, B. A.; Otting, G. *J. Am. Chem. Soc.* **2008**, *130*, 10486.
(15) Keizers, P. H. J.; Saragliadis, A.; Hiruma, Y.; Overhand, M.; Ubbink, M. *J. Am. Chem. Soc.* **2008**, *130*, 14802.
(16) Hass, M. A. S.; Keizers, P. H. J.; Blok, A.; Hiruma, Y.; Ubbink, M. *J. Am. Chem. Soc.* **2010**, *132*, 9952.
(17) Das Gupta, S.; Hu, X.; Keizers, P. H. J.; Liu, W.-M.; Luchinat, C.; Nagulapalli, M.; Overhand, M.; Parigi, G.; Sgheri, L.; Ubbink, M. *J. Biomol. NMR* **2011**, *51*, 253.
(18) Bertini, I.; Calderone, V.; Cerofolini, L.; Fragai, M.; Geraldes, C. F. G. C.; Hermann, P.; Luchinat, C.; Parigi, G.; Teixeira, J. M. C. *FEBS Lett.* **2012**, *586*, 557.
(19) Balayssac, S.; Bertini, I.; Lelli, M.; Luchinat, C.; Maletta, M.; Yeo, K. J. *J. Am. Chem. Soc.* **2007**, *129*, 2218.
(20) Kervern, G.; D'Aléo, A.; Toupet, L.; Maury, O.; Emsley, L.; Pintacuda, G. *Angew. Chem., Int. Ed.* **2009**, *48*, 3082.
(21) Castellani, F.; van Rossum, B.; Diehl, A.; Schubert, M.; Rehbein, K.; Oschkinat, H. *Nature* **2002**, *420*, 98.
(22) Balayssac, S.; Bertini, I.; Bhaumik, A.; Lelli, M.; Luchinat, C. *Proc. Natl. Acad. Sci. U.S.A.* **2008**, *105*, 17284.
(23) Nadaud, P. S.; Helmus, J. J.; Kall, S. L.; Jaroniec, C. P. *J. Am. Chem. Soc.* **2009**, *131*, 8108.
(24) Loquet, A.; Giller, K.; Becker, S.; Lange, A. *J. Am. Chem. Soc.* **2010**, *132*, 15164.
(25) Nadaud, P. S.; Helmus, J. J.; Höfer, N.; Jaroniec, C. P. *J. Am. Chem. Soc.* **2007**, *129*, 7502.
(26) Bertini, I.; Bhaumik, A.; De Paepe, G.; Griffin, R. G.; Lelli, M.; Lewandowski, J. R.; Luchinat, C. *J. Am. Chem. Soc.* **2010**, *132*, 1032.
(27) Bertini, I.; Emsley, L.; Lelli, M.; Luchinat, C.; Mao, J.; Pintacuda, G. *J. Am. Chem. Soc.* **2010**, *132*, 5558.
(28) Bertini, I.; Luchinat, C.; Parigi, G. *Prog. NMR Spectrosc.* **2002**, *40*, 249.
(29) Bertini, I.; Luchinat, C.; Parigi, G.; Pierattelli, R. *ChemBioChem* **2005**, *6*, 1536.
(30) Murshudov, G. N.; Vagin, A. A.; Dodson, E. J. *Acta Crystallogr., Sect. D* **1997**, *53*, 240.
(31) Bertini, I.; Calderone, V.; Cosenza, M.; Fragai, M.; Lee, Y.-M.; Luchinat, C.; Mangani, S.; Terni, B.; Turano, P. *Proc. Natl. Acad. Sci. U.S.A.* **2005**, *102*, 5334.
(32) Cullity, B. D.; Stock, S. R. *Elements of X-Ray Diffraction*, 3rd ed.; Prentice Hall: Upper Saddle River, NJ, 2001.
(33) Margiolaki, I.; Wright, J. P.; Wilmanns, M.; Fitch, A. N.; Pinotsis, N. *J. Am. Chem. Soc.* **2007**, *129*, 11865.
(34) Von Dreele, R. B. *Methods Enzymol.* **2003**, *368*, 254.
(35) Herrmann, T.; Güntert, P.; Wüthrich, K. *J. Mol. Biol.* **2002**, *319*, 209.
(36) Balayssac, S.; Bertini, I.; Luchinat, C.; Parigi, G.; Piccioli, M. *J. Am. Chem. Soc.* **2006**, *128*, 15042.
(37) Matthews, B. W. *J. Mol. Biol.* **1968**, *33*, 491.
(38) Matthews, B. W. *Annu. Rev. Phys. Chem.* **1976**, *27*, 493.
(39) For the structure based on the wrong $P2_12_12_1$ symmetry, the BB RMSD to the mean was 1.1 Å, and the RMSD to the X-ray structure was 1.4 Å (Table 1, entry 4). Although the symmetry-related molecules are incorrectly positioned, the calculated structural family is very close to the structural family calculated with the correct symmetry (see Figures S3 and S4).